

# Stochasticity in radiative polarization of ultrarelativistic electrons in an ultrastrong laser pulse

Ren-Tong Guo,<sup>1,2,\*</sup> Yu Wang,<sup>1,2,\*</sup> Rashid Shaisultanov,<sup>2</sup> Feng Wan,<sup>1</sup> Zhong-Feng Xu,<sup>1</sup> Yue-Yue Chen,<sup>3,2,†</sup> Karen Z. Hatsagortsyan,<sup>2,‡</sup> and Jian-Xing Li<sup>1,2,§</sup>

<sup>1</sup>*MOE Key Laboratory for Nonequilibrium Synthesis and Modulation of Condensed Matter, School of Science, Xi'an Jiaotong University, Xi'an 710049, China*

<sup>2</sup>*Max-Planck-Institut für Kernphysik, Saupfercheckweg 1, 69117 Heidelberg, Germany*

<sup>3</sup>*Department of Physics, Shanghai Normal University, Shanghai 200234, China*

(Dated: March 26, 2020)

Stochasticity effects in the spin (de)polarization of an ultrarelativistic electron beam during photon emissions in a counterpropagating ultrastrong focused laser pulse in the quantum radiation reaction regime are investigated. We employ a Monte Carlo method to describe the electron dynamics semiclassically, and photon emissions as well as the electron radiative polarization quantum mechanically. While in the latter the photon emission is inherently stochastic, we were able to identify its imprints in comparison with the new developed semiclassical stochasticity-free method of radiative polarization applicable in the quantum regime. With an initially spin-polarized electron beam, the stochastic spin effects are seen in the dependence of the depolarization degree on the electron scattering angle and the electron final energy (spin stochastic diffusion). With an initially unpolarized electron beam, the spin stochasticity is exhibited in enhancing the known effect of splitting of the electron beam along the propagation direction into two oppositely polarized parts by an elliptically polarized laser pulse. The considered stochasticity effects for the spin are observable with currently achievable laser and electron beam parameters.

The modern ultrastrong laser technique [1–7] allows for investigation of nonlinear QED processes [8–10] and radiation reaction effects [11–15]. Thus, recently classical and quantum signatures of radiation reaction in the electron energy losses have been identified in the experiments of an ultrarelativistic electron beam collision with strong laser fields [16, 17]. Quantum features of radiation reaction originate from the discrete and probabilistic character of a photon emission, which gives rise to stochasticity effects. The latter is responsible for the broadening of the energy spread of an electron beam in a plane laser field [18–20], causes electron stochastic heating in a standing laser field [21], results in quantum quenching of radiation losses in short laser pulses [22], disturbs the angular distribution of radiation [23, 24], and brings about the so-called electron straggling effect [25, 26], when the electron propagates a long distance without radiation, resulting in the increase of the yield of high-energy photons. Radiation reaction can have impact on the electron spin dynamics, proved since long ago for synchrotron radiation. It may induce polarization of the unpolarized electron beams (Sokolov-Ternov effect) [27–30], or depolarization of the initially polarized beam [31, 32].

Polarized electrons are commonly generated either by accelerating nonrelativistic polarized electrons, obtained from photocathodes [33], spin filters [34] and beam splitters [35], by conventional accelerators [36] and laser wakefield accelerators [37, 38], or by radiative polarization in storage rings [39, 40], in which the polarization typically requires a period from minutes to hours because of the modest magnetic fields in storage rings  $\sim$  Tesla. Recently, there are several proposals on how to use ultrastrong laser fields for generation of po-

larized relativistic electron beams [41–49]. In particular, the possibilities for creation of ultrarelativistic high-polarization high-density electron and positron beams in femtoseconds via utilizing asymmetric spin-dependent radiation reaction in elliptically polarized laser fields are shown in [44–46], and using two-color laser fields in [47–49]. The methods put forward in these works open a door for detailed investigation of all features of the radiative polarization and depolarization processes in ultrastrong focused laser fields, as well as in multiple laser beam configurations. Usually, a full quantum mechanical study of radiation reaction includes all quantum effects, such as the photon recoil, stochasticity, and interferences, which makes difficult to single out the specific radiation reaction signatures of the stochasticity.

In this work, stochasticity effects in radiative (de)polarization of an ultrarelativistic electron beam head-on colliding with an ultrastrong laser pulse are investigated in the quantum radiation reaction regime; see the interaction scenarios in Fig. 1. We employ a Monte Carlo (MC) method to describe spin-resolved electron dynamics in a strong laser field, stochastic photon emissions, and corresponding stochastic radiative spin evolution. To elucidate the role of stochastic spin effects, we develop an auxiliary semiclassical stochasticity-free (SF) method for the description of the spin-dependent radiation reaction on the electron dynamics. For this purposes we use the Baier-Katkov-Strakhovenko equation for the expectation value of the electron spin [30, 50], which is a generalization of the Thomas-Bargmann-Michel-Telegdi (TBMT) equation [51–53], including radiation reaction for the electron spin. The latter is supplemented with the modified Landau-Lifshitz equation [44], including the spin-dependent radiation reaction and the quantum recoil. Firstly, we consider a depolarization scenario for the initially longitudinally spin-polarized (LSP) (along velocity,  $z$ -axis) electron beam. The depolarization proceeds in different ways in semiclassical and quantum models, which after the interaction yields differences in

\* These authors have contributed equally to this work.

† yueyuechen@shnu.edu.cn

‡ k.hatsagortsyan@mpi-hd.mpg.de

§ jianxing@xjtu.edu.cn

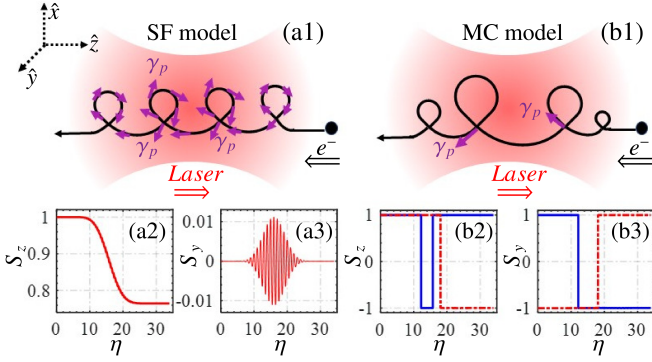


FIG. 1. Scenario for the detection of stochasticity effects in radiative depolarization. The trajectories and spin evolutions of LSP electrons head-on colliding with a linearly polarized laser pulse, polarizing in  $x$  direction and propagating along  $+z$  direction: (a1)-(a3) in the SF model and (b1)-(b3) in the MC model.  $S_\alpha$  is the spin component measured along the  $\alpha$ -axis,  $\alpha = \{x, y, z\}$ ,  $e^-$  and  $\gamma_p$  indicate the electron and emitted photon, respectively, red-dashed and blue-solid curves in (b2) and (b3) two different sample electron, respectively, and  $\eta$  the laser phase.

the angle-resolved polarization distribution of the electron beam, and provides the stochasticity signatures for the spin radiative dynamics. In particular, in the SF model an electron continuously loses energies due to radiation (without stochastic effects and straggling in photon emissions, the photon energies are typically low), which gradually alter the electron trajectory and the spin longitudinal component due to radiation reaction, while the spin component along the laser magnetic field oscillates in the symmetric laser field, as shown in Figs. 1(a1)-(a3). On the contrary, in the MC model a finite number of photons are stochastically emitted with random energies and discretely alter the electron dynamics due to the quantum recoil, and the quantum spin state stochastically flips on the instantaneous spin quantization axis (SQA), see Figs. 1(b1)-(b3). The signatures of the stochasticity are identified by analyzing the features of the stochastic spin diffusion. In the second applied scenario, we use an initially unpolarized electron beam head-on colliding with an elliptically polarized laser pulse. Here, the unpolarized electron beam splits along the propagation direction into two oppositely polarized parts, and the stochasticity effect is observed in enhancing the separation.

We employ ultrastrong laser fields with the invariant field parameter  $a_0 \equiv eE_0/(m\omega_0) \gg 1$  [54, 55], where  $E_0$  and  $\omega_0$  are the laser field amplitude and frequency, respectively, and  $-e$  and  $m$  the electron charge and mass, respectively. Relativistic units with  $c = \hbar = 1$  are used throughout. The quantum radiation reaction regime requires the invariant quantum parameter  $\chi \equiv |e| \sqrt{-(F_{\mu\nu}p^\nu)^2}/m^3 \gtrsim 1$  [54, 55], with the field tensor  $F_{\mu\nu}$  and the four-vector of the electron momentum  $p^\nu$ . In the electron-laser counterpropagating scheme,  $\chi \approx 2a_0\gamma_e\omega_0/m$ , with the electron Lorentz factor  $\gamma_e$ .

In the MC method, we treat spin-resolved electron dynamics semiclassically and photon emissions quantum mechanically in the local constant field approximation [54–57], valid at  $a_0 \gg 1$ . At each simulation step, the photon emission is calculated

following the common algorithms [58–60] and the photon polarization, represented by the Stokes parameters  $(\xi_1, \xi_2, \xi_3)$  [61], is calculated according to our MC algorithm introduced in Refs. [62, 63]; see also [64]. After the photon emission the electron spin state is determined by the spin-resolved emission probabilities, derived in the QED operator method of Baier-Katkov [65], and instantaneously collapsed into one of its basis states defined with respect to the instantaneous SQA, which is chosen according to the particular observable of interest: to determine the polarization of the electron along the magnetic field in its rest frame, the SQA is chosen along the magnetic field  $\mathbf{n}_B = \boldsymbol{\beta} \times \hat{\mathbf{a}}$  with the scaled electron velocity  $\boldsymbol{\beta} = \mathbf{v}/c$  and the unit vector  $\hat{\mathbf{a}} = \mathbf{a}/|\mathbf{a}|$  along the electron acceleration  $\mathbf{a}$  [44, 47]. In the case when the electron beam is initially polarized with the initial spin vector  $\mathbf{S}_i$ , the observable of interest is the spin expectation value along the initial polarization and the SQA is chosen along that direction [64]. Between photon emissions, the spin precession is governed by TBMT equation:

$$\left(\frac{d\mathbf{S}}{d\eta}\right)_T = \frac{e\gamma_e}{(k \cdot p_i)} \mathbf{S} \times \left[ -\left(\frac{g}{2} - 1\right) \frac{\gamma_e}{\gamma_e + 1} (\boldsymbol{\beta} \cdot \mathbf{B}) \cdot \boldsymbol{\beta} + \left(\frac{g}{2} - 1 + \frac{1}{\gamma_e}\right) \mathbf{B} - \left(\frac{g}{2} - \frac{\gamma_e}{\gamma_e + 1}\right) \boldsymbol{\beta} \times \mathbf{E} \right], \quad (1)$$

where  $\mathbf{E}$  and  $\mathbf{B}$  are the laser electric and magnetic fields, respectively,  $\eta = k \cdot r$  the laser phase,  $p_i$ ,  $k$ , and  $r$  4-vectors of the electron momentum before radiation, laser wave vector, and coordinate, respectively, and  $g$  the electron gyromagnetic factor [64]. The simulation results of the electron spin dynamics with our method concur with those of the CAIN code [66].

In our SF method, we revise the TBMT equation, including a term responsible for radiation reaction. For the revision we generalize for arbitrary  $\chi$  the method of Refs. [30, 50], where radiation reaction for the spin evolution is calculated at  $\chi \ll 1$ . Thus, the equation which is used for the spin evolution including radiation reaction reads:

$$\frac{d\mathbf{S}}{d\eta} = \left(\frac{d\mathbf{S}}{d\eta}\right)_T - P [\psi_1(\chi)\mathbf{S} + \psi_2(\chi)(\mathbf{S} \cdot \boldsymbol{\beta})\boldsymbol{\beta} + \psi_3(\chi)\mathbf{n}_B], \quad (2)$$

where  $P = \alpha m^2 / [\sqrt{3}\pi(k \cdot p_i)]$ ,  $\psi_1(\chi) = \int_0^\infty u'' du K_{\frac{2}{3}}(u')$ ,  $\psi_2(\chi) = \int_0^\infty u'' du \int_{u'}^\infty dx K_{\frac{1}{3}}(x) - \psi_1(\chi)$ ,  $\psi_3(\chi) = \int_0^\infty u'' du K_{\frac{1}{3}}(u')$ ,  $u' = 2u/3\chi$ ,  $u'' = u^2/(1+u)^3$ ,  $u = \varepsilon_\gamma/(\varepsilon_i - \varepsilon_\gamma)$ ,  $\varepsilon_i$  and  $\varepsilon_\gamma$  are the electron energy before radiation and emitted photon energy, respectively, and  $K_n$  the  $n$ -order modified Bessel function of the second kind. Further, in the SF method the electron dynamics is described by the Landau-Lifshitz equation [67] with corrections for the quantum recoil [68], and the photon polarization is calculated by the average method as in [62]. The validity, comparison and more details on MC and SF methods are given in [64].

The angle- and energy-resolved distributions of the polarization and density of the electron beam are illustrated in Fig. 2, including and excluding radiative stochasticity, calculated by the MC and SF methods, respectively. Employed laser and electron beam parameters are as follows. A realistic tightly-focused Gaussian linearly polarized laser pulse [64, 69] propagates along  $+z$  direction (polar angle  $\theta_l = 0^\circ$ ), with peak

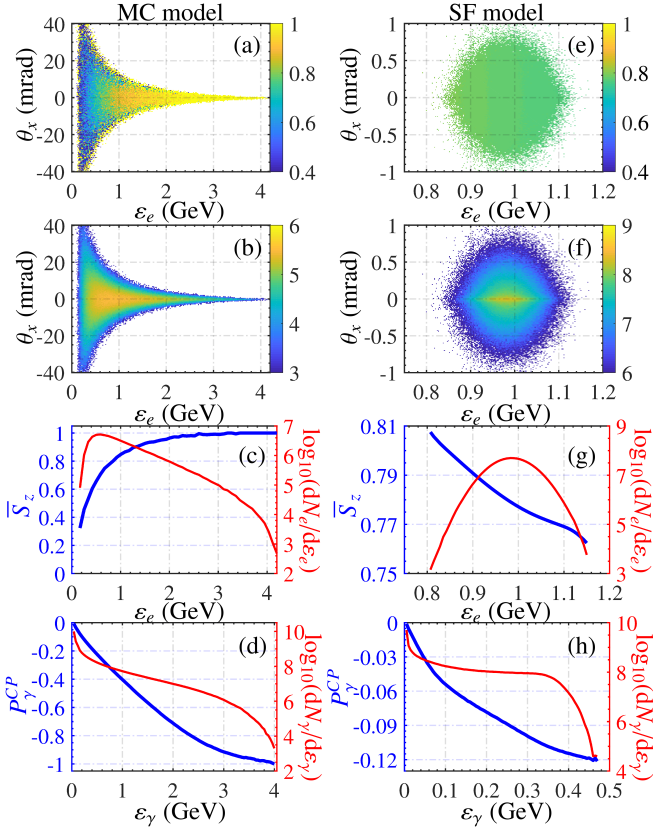


FIG. 2. (a) and (e): Longitudinal average spin (polarization)  $\bar{S}_z$  vs the deflection angle  $\theta_x = \arctan(p_x/p_z)$  and the electron energy  $\varepsilon_e$ . (b) and (f): Angle-resolved electron density  $\log_{10}(d^2N_e/d\theta_x d\varepsilon_e)$  ( $\text{mrad}^{-1} \cdot \text{GeV}^{-1}$ ). (c) and (g):  $\bar{S}_z$  (blue, calculated by summing over  $\theta_x$  in (a) and (e), respectively) and  $\log_{10}(dN_e/d\varepsilon_e)$  (red, calculated by summing over  $\theta_x$  in (b) and (f), respectively) vs  $\varepsilon_e$ . (d) and (h): Degree of circular polarization of emitted photons  $P_y^{CP} = \xi_2$  [61, 62] (blue) and energy density  $\log_{10}(dN_\gamma/d\varepsilon_\gamma)$  (red) vs the photon energy  $\varepsilon_\gamma$ . The left and right columns indicate the cases including and excluding radiative stochasticity, calculated by the MC and SF methods, respectively. The laser and electron beam parameters are given in the text.

intensity  $I_0 \approx 3.45 \times 10^{21} \text{ W/cm}^2$  ( $a_0 = 50$ ), wavelength  $\lambda_0 = 1 \mu\text{m}$ , pulse duration  $\tau = 10T_0$  with period  $T_0$ , and focal radius  $w_0 = 5 \mu\text{m}$ . The counterpropagating LSP electron beam has a cylindrical form, with average spin (polarization) components  $(\bar{S}_x, \bar{S}_y, \bar{S}_z) = (0, 0, 1)$ , polar angle  $\theta_e = 180^\circ$ , azimuthal angle  $\phi_e = 0^\circ$ , radius  $w_e = \lambda_0$ , length  $L_e = 5\lambda_0$ , electron number  $N_e = 5 \times 10^6$  (density  $n_e \approx 3.18 \times 10^{17} \text{ cm}^{-3}$  with a transversely Gaussian and longitudinally uniform distribution), initial kinetic energy  $\varepsilon_0 = 4 \text{ GeV}$  (the maximum value of the quantum parameter during the interaction is  $\chi_{max} \approx 1.89$ ), angular divergence  $\Delta\theta = 0.3 \text{ mrad}$ , energy spread  $\Delta\varepsilon_0/\varepsilon_0 = 0.06$ , and emittance  $\varepsilon_e \approx 3 \times 10^{-4} \text{ mm}\cdot\text{mrad}$ . Such electron beams are achievable via laser wakefield acceleration [70, 71] with further radiative polarization [44, 48, 49], or alternatively, via directly wakefield acceleration of LSP electrons [37, 38].

Radiative stochasticity induces very broad angular and energy distributions in the MC model in comparison with the SF case, cf. panels (a)–(b) with (e)–(f) in Fig. 2. The spreads are particularly large in the laser polarization direction. The

spin and density distributions of the electrons are demonstrated more visibly for the MC model in Fig. 2(c), by summing over  $\theta_x$  in Figs. 2(a) and (b), respectively. The electron energies after the interaction are distributed in the MC simulation in a rather large range from 0.2 to 4.2 GeV, because due to the straggling effects some electrons do not radiate much. The average spin polarization  $\bar{S}_z$  monotonically increases with the energy from approximately 34% up to 100%. This is because more photon emissions lead to more energy losses, and more radiation reaction to more spin flips and further larger depolarization.

In contrast to that, in the SF model the final electron energies have relatively small spread approximately from 0.81 GeV to 1.15 GeV. The  $\bar{S}_z$  behaviour is qualitatively opposite to the MC model, it monotonically decreases with the energy increase, but the variation is not large, approximately from 80.7% to 76.4%, as shown in Fig. 2(g). We analyze the reason for the polarization behaviour with the help of Fig. 3. First of all, let us note that the electrons in the beam experience similar instantaneous laser fields because the applied waist-size of the beam is not small  $w_0 = 5w_e$ ; see the fields experienced by three sample electrons in Fig. 3(b). Then, the electron dynamics are gradually altered by continuous similar photon emissions. The relation of the polarization to the energy during the interaction is shown in Fig. 3(a). For the electron with a larger initial energy (see the sample electron “ $e_3$ ” in Fig. 3(a)), the radiation is stronger due to the larger parameter  $\chi \sim a_0\gamma_e$ , and consequently, the depolarization is larger, but its final energy is still higher, because the radiative energy loss is smaller than the initial energy spread.

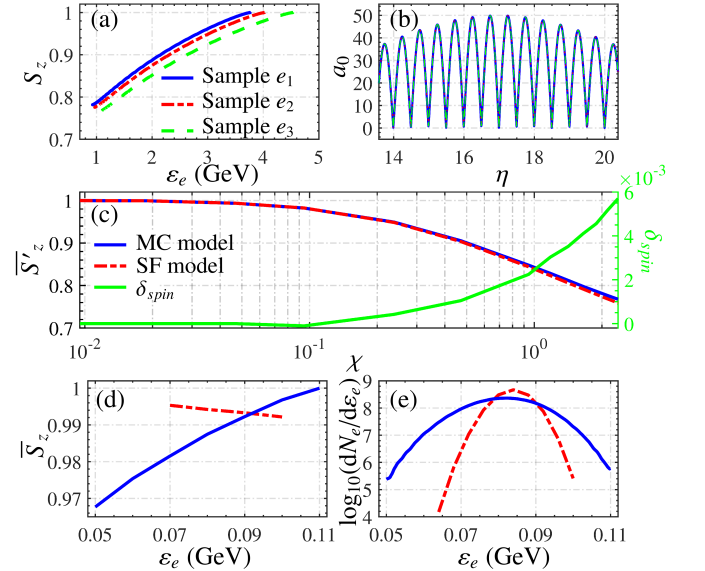


FIG. 3. (a) and (b): Instantaneous  $S_z$  vs  $\varepsilon_e$  and experienced  $a_0$  vs  $\eta$  for three sample electrons, respectively, simulated by the SF method. The sample electrons are chosen with randomly spatial coordinates and different energies. (c) The variation of the average polarization of all electrons  $\bar{S}'_z$  and the relative deviation  $\delta_{spin}$  with respect to  $\chi$ . (d) and (e):  $\bar{S}_z$  and  $\log_{10}(dN_e/d\varepsilon_e)$  vs  $\varepsilon_e$ , respectively, for the case of  $\chi \approx 0.047$ . In (c)–(e), the blue-solid and red-dashed curves are simulated by the MC and SF methods, respectively. Other laser and electron beam parameters are the same with those in Fig. 2.

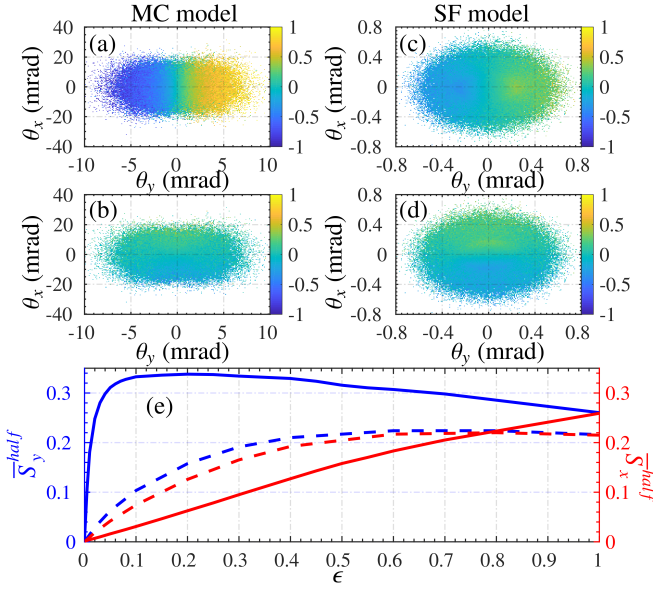


FIG. 4. Transverse polarization of the initially unpolarized electron beam after the interaction with elliptically polarized laser field: (a) and (b) [(c) and (d)]: Transverse polarization components  $\bar{S}_y$  and  $\bar{S}_x$  vs the deflection angles  $\theta_x$  and  $\theta_y = \arctan(p_y/p_z)$ , respectively, simulated by the MC [SF] method with the laser ellipticity  $\epsilon = |E_y|/|E_x| = 0.2$ . (e) Average transverse polarization  $\bar{S}_y^{half}$  (calculated by summing  $\bar{S}_y$  over  $\theta_y > 0$  and  $\theta_x$  in (a) and (c) for the MC (blue-solid) and SF (blue-dashed) methods, respectively) and  $\bar{S}_x^{half}$  (calculated by summing  $\bar{S}_x$  over  $\theta_x > 0$  and  $\theta_y$  in (b) and (d) for the MC (red-solid) and SF (red-dashed) methods, respectively) vs  $\epsilon$ . Other laser and electron beam parameters are the same as in Fig. 2.

The average polarization of all electrons  $\bar{S}'_z$  in the MC and SF models are comparable,  $\bar{S}'_z^{MC} \approx 78.64\%$  and  $\bar{S}'_z^{SF} \approx 77.92\%$ , respectively, derived from data of Figs. 2(c) and (g). The relative deviation is  $\delta_{spin} = (\bar{S}'_z^{MC} - \bar{S}'_z^{SF}) / (\bar{S}'_z^{MC} + \bar{S}'_z^{SF}) \approx 0.46\%$ . The variation of  $\bar{S}'_z$  with respect to the quantum parameter  $\chi$  is shown in Fig. 3(c), which confirms that the SF method can provide the average depolarization (polarization) degree quite accurately, with a relative error of  $\delta_{spin} < 1\%$  at  $\chi \lesssim 2$ . With increasing  $\chi$ , the stochasticity effects become larger and  $\delta_{spin}$  raises. Although, at rather low  $\chi \approx 0.047$ , when the stochasticity is very weak, the average polarization can be deduced from the SF model, but the detailed energy-resolved polarization and density still show differences with respect to the stochastic MC model, as shown in Figs. 3(d) and (e). Thus, the rising behavior of the electron polarization with the energy increase in the electron beam after the interaction [cf. panel (c) with (g) in Fig. 2] is a distinct signature of the stochasticity in the radiative depolarization process. Note that the polarization of employed high-energy high-density electron beams can be detected by the linear or nonlinear Compton scattering [46, 72].

We have investigated also the role of stochasticity effects for emitted high-energy highly circularly-polarized  $\gamma$ -rays; see Figs. 2(d) and (h). While the circular polarization degree of  $\gamma$ -photons varies with energy in a rather large range approximately from 0 to -1 in the MC model, the SF model shows

much smaller range approximately from 0 to -0.1. However, the average polarization degrees are similar and low, about -0.077 and -0.081 for the MC and SF models, respectively. This is because in the MC model the polarization is high for high-energy photons with very low numbers, see Figs. 2(d)-(h). The energy range of  $\gamma$ -photons is much larger in the MC model, similar to the electron energy distribution, which yields generation of high-energy high-brilliance highly circularly-polarized  $\gamma$ -rays, as discussed in [62].

Now we turn to the discussion of the case of initially unpolarized electron beam and look for the stochasticity effects in the spin dynamics. It is known [44] that an initially unpolarized electron beam can be split into two oppositely polarized parts during interaction with a counterpropagating elliptically polarized laser pulse (the minor axis along  $y$  direction). We have analyzed this polarization-dependent splitting effect with the MC and SF models for the full range of the ellipticity; see Fig. 4. Exemplary distributions of the transverse polarization components with respect to the electron deflection angle after the interaction in the case of  $\epsilon = 0.2$  are shown in Figs. 4(a)-(d), calculated within the MC and SF models, respectively. In both models the electron beam splits into two parts along the propagation direction, which are oppositely polarized. At small ellipticity, the electron spin-polarization along the minor axis of the ellipticity is the largest, with small angular separation along that axis. The separated half of the electron beam (e.g.  $\theta_y > 0$ ) has an average polarization (e.g.  $\bar{S}_y^{half}$ ), which depends on the separation angle: the larger separation angle, the larger the average polarization  $\bar{S}_y^{half}$ . In the MC model the separation angle is significantly larger than that in the SF case due to stochasticity (as in this case photons of larger energies are emitted), and consequently  $\bar{S}_y^{half}$  is larger; see Fig. 4(e). The deviation of  $\bar{S}_y^{half}$  between the MC and SF models is the largest at small ellipticity near 0.05 for the given parameters. In the MC model of Fig. 4(a)  $|\bar{S}_y^{half}| \approx 33.8\%$ , by comparison in the SF model of Fig. 4(c)  $|\bar{S}_y^{half}| \approx 15.8\%$  is much lower. While in the SF model  $\bar{S}_x^{half}$  and  $\bar{S}_y^{half}$  increase monotonously with the increase of the ellipticity, in the MC model  $\bar{S}_y^{half}$  demonstrates a characteristic nonmonotonic behavior with a peak at small ellipticity. The latter can serve as a signature of the stochasticity effects in radiative polarization of initially unpolarized electron beams.

For the experimental feasibility, we have investigated the impact of the laser and electron beam parameters, e.g., variations of  $\epsilon_0$ ,  $a_0$  and  $\tau$ , larger energy spread of 10%, larger angular divergence of 1 mrad, larger colliding angle of  $\theta_e = 175^\circ$  and initial transversely spin-polarization of the electron beam, on the considered signatures of radiative stochasticity, and the results keep uniform [64].

In conclusion, we have analyzed the impact of stochastic photon emission in a strong laser field on the initially LSP electron radiative depolarization as well as on the emitted  $\gamma$ -ray polarization. The qualitative signatures of the stochasticity have been demonstrated in the energy-resolved electron polarization after the interaction and in the energy-resolved

polarization of the emitted  $\gamma$ -photons. In the case of initially unpolarized electron beam, the stochasticity effect is demonstrated in the dependence of the electron polarization on the laser ellipticity. These qualitative signatures are observable with the currently available laser facilities.

*Acknowledgement:* R.-T. Guo, Y. Wang and J.-X. Li thank Prof. C. Keitel for hospitality. This work is supported by the National Natural Science Foundation of China (Grants Nos. 11874295, 11875219 and 11905169), and the National Key R&D Program of China (Grant No. 2018YFA0404801).

- 
- [1] Colin N. Danson, Constantin Haefner, Jake Bromage, Thomas Butcher, Jean-Christophe F. Chanteloup, Enam A. Chowdhury, Almantas Galvanauskas, Leonida A. Gizzi, Joachim Hein, David I. Hillier, and et al., “Petawatt and exawatt class lasers worldwide,” *High Power Laser Sci. Eng.* **7**, e54 (2019).
- [2] Jin Woo Yoon, Cheonha Jeon, Junghoon Shin, Seong Ku Lee, Hwang Woon Lee, Il Woo Choi, Hyung Taek Kim, Jae Hee Sung, and Chang Hee Nam, “Achieving the laser intensity of  $5.5 \times 10^{22}$  w/cm<sup>2</sup> with a wavefront-corrected multi-pw laser,” *Opt. Express* **27**, 20412–20420 (2019).
- [3] S. Gales, K. A. Tanaka, D. L. Balabanski, F. Negoita, D. Stutman, O. Tesileanu, C. A. Ur, D. Ursescu, I. An-drei, S. Ataman, M. O. Cernaianu, L. DAlessi, I. Dancus, B. Diaconescu, N. Djourelou, D. Filipescu, P. Ghenuche, D. G. Ghita, C. Matei, K. Seto, M. Zeng, and N. V. Zamfir, “The extreme light infrastructure nuclear physics (eli-np) facility: new horizons in physics with 10 pw ultra-intense lasers and 20 mev brilliant gamma beams,” *Rep. Prog. Phys.* **81**, 094301 (2018).
- [4] The Extreme Light Infrastructure (ELI), <http://www.eli-beams.eu/en/facility/lasers/>.
- [5] The Vulcan facility, <http://www.clf.stfc.ac.uk/Pages/The-Vulcan-10-Petawatt-Project.aspx>.
- [6] Exawatt Center for Extreme Light Studies (XCELS), <http://www.xcels.iapras.ru/>.
- [7] The Center for Relativistic Laser Science (CoReLS), [https://www.ibs.re.kr/eng/sub02\\_03\\_05.do](https://www.ibs.re.kr/eng/sub02_03_05.do).
- [8] C. Bula, K. T. McDonald, E. J. Prebys, C. Bamber, S. Boege, T. Kotseroglou, A. C. Melissinos, D. D. Meyerhofer, W. Ragg, D. L. Burke, R. C. Field, G. Horton-Smith, A. C. Odian, J. E. Spencer, D. Walz, S. C. Berridge, W. M. Bugg, K. Shmakov, and A. W. Weidemann, “Observation of nonlinear effects in Compton scattering,” *Phys. Rev. Lett.* **76**, 3116–3119 (1996).
- [9] D. L. Burke, R. C. Field, G. Horton-Smith, J. E. Spencer, D. Walz, S. C. Berridge, W. M. Bugg, K. Shmakov, A. W. Weidemann, C. Bula, K. T. McDonald, E. J. Prebys, C. Bamber, S. J. Boege, T. Koffas, T. Kotseroglou, A. C. Melissinos, D. D. Meyerhofer, D. A. Reis, and W. Ragg, “Positron production in multiphoton light-by-light scattering,” *Phys. Rev. Lett.* **79**, 1626 (1997).
- [10] I. C. E. Turcu, B. Shen, D. Neely, G. Sarri, K. A. Tanaka, P. McKenna, S. P. D. Mangles, T.-P. Yu, W. Luo, X.-L. Zhu, and et al., “Quantum electrodynamics experiments with colliding petawatt laser pulses,” *High Power Laser Sci. Eng.* **7**, e10 (2019).
- [11] M. Abraham, *Theorie der Elektrizität* (Teubner, Leipzig, 1905).
- [12] H. A. Lorentz, *The Theory of Electrons* (Teubner, Leipzig, 1909).
- [13] P. A. M. Dirac, “Classical theory of radiating electrons,” *Proc. Roy. Soc. (London)* **A167**, 148 (1938).
- [14] W. Heitler, “The influence of radiation damping on the scattering of light and mesons by free particles,” *Math. Proc. Camb. Phil. Soc.* **37**, 291 (1941).
- [15] A. Di Piazza, C. Müller, K. Z. Hatsagortsyan, and C. H. Keitel, “Extremely high-intensity laser interactions with fundamental quantum systems,” *Rev. Mod. Phys.* **84**, 1177 (2012).
- [16] J. M. Cole, K. T. Behm, E. Gerstmayr, T. G. Blackburn, J. C. Wood, C. D. Baird, M. J. Duff, C. Harvey, A. Ilderton, A. S. Joglekar, K. Krushelnick, S. Kuschel, M. Marklund, P. McKenna, C. D. Murphy, K. Poder, C. P. Ridgers, G. M. Samarin, G. Sarri, D. R. Symes, A. G. R. Thomas, J. Warwick, M. Zepf, Z. Najmudin, and S. P. D. Mangles, “Experimental evidence of radiation reaction in the collision of a high-intensity laser pulse with a laser-wakefield accelerated electron beam,” *Phys. Rev. X* **8**, 011020 (2018).
- [17] K. Poder, M. Tamburini, G. Sarri, A. Di Piazza, S. Kuschel, C. D. Baird, K. Behm, S. Bohlen, J. M. Cole, D. J. Corvan, M. Duff, E. Gerstmayr, C. H. Keitel, K. Krushelnick, S. P. D. Mangles, P. McKenna, C. D. Murphy, Z. Najmudin, C. P. Ridgers, G. M. Samarin, D. R. Symes, A. G. R. Thomas, J. Warwick, and M. Zepf, “Experimental signatures of the quantum nature of radiation reaction in the field of an ultraintense laser,” *Phys. Rev. X* **8**, 031004 (2018).
- [18] N. Neitz and A. Di Piazza, “Stochasticity effects in quantum radiation reaction,” *Phys. Rev. Lett.* **111**, 054802 (2013).
- [19] N. Neitz and A. Di Piazza, “Electron-beam dynamics in a strong laser field including quantum radiation reaction,” *Phys. Rev. A* **90**, 022102 (2014).
- [20] Samuel R. Yoffe, Yevgen Kravets, Adam Noble, and Dino A. Jaroszynski, “Longitudinal and transverse cooling of relativistic electron beams in intense laser pulses,” *New J. Phys.* **17**, 053025 (2015).
- [21] A. V. Bashinov, A. V. Kim, and A. M. Sergeev, “Impact of quantum effects on relativistic electron motion in a chaotic regime,” *Phys. Rev. E* **92**, 043105 (2015).
- [22] C. N. Harvey, A. Gonoskov, A. Ilderton, and M. Marklund, “Quantum quenching of radiation losses in short laser pulses,” *Phys. Rev. Lett.* **118**, 105004 (2017).
- [23] A. Di Piazza, K. Z. Hatsagortsyan, and C. H. Keitel, “Quantum radiation reaction effects in multiphoton Compton scattering,” *Phys. Rev. Lett.* **105**, 220403 (2010).
- [24] Jian-Xing Li, Yue-Yue Chen, Karen Z. Hatsagortsyan, and Christoph H. Keitel, “Angle-resolved stochastic photon emission in the quantum radiation-dominated regime,” *Sci. Rep.* **7** (2017).
- [25] C. S. Shen and D. White, “Energy straggling and radiation reaction for magnetic bremsstrahlung,” *Phys. Rev. Lett.* **28**, 455–459 (1972).
- [26] T. G. Blackburn, C. P. Ridgers, J. G. Kirk, and A. R. Bell, “Quantum radiation reaction in laserelectron-beam collisions,” *Phys. Rev. Lett.* **112**, 015001 (2014).
- [27] A. A. Sokolov and I. M. Ternov, *Sov. Phys. Dokl.* **8**, 1203 (1964).
- [28] A. A. Sokolov and I. M. Ternov, *Synchrotron Radiation* (Akademik, Germany, 1968).
- [29] V. N. Baier and V. M. Katkov, “Radiational polarization of electrons in inhomogeneous magnetic field,” *Phys. Lett. A* **24**, 327–329 (1967).
- [30] V. N. Baier, “Radiative polarization of electron in storage rings,”

- Sov. Phys. Usp. **14**, 695 (1972).
- [31] Ya. S. Derbenev and A. M. Kondratenko, "Diffusion of particle spins in storage rings," Sov. Phys. JETP **35**, 230–236 (1972).
- [32] K. Heinemann and D. P. Barber, "Spin transport, spin diffusion and bloch equations in electron storage rings," Nucl. Instrum. Methods Phys. Res., Sect. A **463**, 62–67 (2001).
- [33] Daniel T. Pierce and Felix Meier, "Photoemission of spin-polarized electrons from gaas," Phys. Rev. B **13**, 5484–5500 (1976).
- [34] H. Batelaan, A. S. Green, B. A. Hitt, and T. J. Gay, "Optically pumped electron spin filter," Phys. Rev. Lett. **82**, 4216–4219 (1999).
- [35] Matthias M. Dellweg and Carsten Müller, "Spin-polarizing interferometric beam splitter for free electrons," Phys. Rev. Lett. **118**, 070403 (2017).
- [36] M. L. Swartz, "Physcs with polarized electron beam," SLAC-PUB-4656 (1988).
- [37] Meng Wen, Matteo Tamburini, and Christoph H. Keitel, "Polarized laser-wakefield-accelerated kiloampere electron beams," Phys. Rev. Lett. **122**, 214801 (2019).
- [38] Yitong Wu, Liangliang Ji, Xuesong Geng, Qin Yu, Nengwen Wang, Bo Feng, Zhao Guo, Weiqing Wang, Chengyu Qin, Xue Yan, Lingang Zhang, Johannes Thomas, Anna Hützen, Markus Büscher, Peter Rakitzis, Alexander Pukhov, Baifei Shen, and Ruxin Li, "Polarized electron-beam acceleration driven by vortex laser pulses," New J. Phys. **21**, 073052 (2019).
- [39] Y. Derbenev and A. M. Kondratenko, "Polarization kinematics of particles in storage rings," Sov. Phys. JETP **37**, 968 (1973).
- [40] S. R. Mane, "Electron-spin polarization in high-energy storage rings. I. Derivation of the equilibrium polarization," Phys. Rev. A **36**, 105 (1987).
- [41] D. Del Sorbo, D. Seipt, T. G. Blackburn, A. G. R. Thomas, C. D. Murphy, J. G. Kirk, and C. P. Ridgers, "Spin polarization of electrons by ultraintense lasers," Phys. Rev. A **96**, 043407 (2017).
- [42] D. Del Sorbo, D. Seipt, A. G. R. Thomas, and C. P. Ridgers, "Electron spin polarization in realistic trajectories around the magnetic node of two counter-propagating, circularly polarized, ultra-intense lasers," Plasma Phys. Control. Fusion **60**, 064003 (2018).
- [43] D. Seipt, D. Del Sorbo, C. P. Ridgers, and A. G. R. Thomas, "Theory of radiative electron polarization in strong laser fields," Phys. Rev. A **98**, 023417 (2018).
- [44] Yan-Fei Li, Rashid Shaisultanov, Karen Z. Hatsagortsyan, Feng Wan, Christoph H. Keitel, and Jian-Xing Li, "Ultrarelativistic electron-beam polarization in single-shot interaction with an ultraintense laser pulse," Phys. Rev. Lett. **122**, 154801 (2019).
- [45] Feng Wan, Rashid Shaisultanov, Yan-Fei Li, Karen Z. Hatsagortsyan, Christoph H. Keitel, and Jian-Xing Li, "Ultrarelativistic polarized positron jets via collision of electron and ultraintense laser beams," Phys. Lett. B **800**, 135120 (2020).
- [46] Yan-Fei Li, Ren-Tong Guo, Rashid Shaisultanov, Karen Z. Hatsagortsyan, and Jian-Xing Li, "Electron polarimetry with nonlinear compton scattering," Phys. Rev. Applied **12**, 014047 (2019).
- [47] Yue-Yue Chen, Pei-Lun He, Rashid Shaisultanov, Karen Z. Hatsagortsyan, and Christoph H. Keitel, "Polarized positron beams via intense two-color laser pulses," Phys. Rev. Lett. **123**, 174801 (2019).
- [48] Huai-Hang Song, Wei-Min Wang, Jian-Xing Li, Yan-Fei Li, and Yu-Tong Li, "Spin-polarization effects of an ultrarelativistic electron beam in an ultraintense two-color laser pulse," Phys. Rev. A **100**, 033407 (2019).
- [49] Daniel Seipt, Dario Del Sorbo, Christopher P. Ridgers, and Alec G. R. Thomas, "Ultrafast polarization of an electron beam in an intense bichromatic laser field," Phys. Rev. A **100**, 061402(R) (2019).
- [50] V. N. Baier, V. M. Katkov, and V. M. Strakhovenko, "Kinetics of radiative polarization," Sov. Phys. JETP **31**, 908 (1970).
- [51] L. H. Thomas, "The motion of the spinning electron," Nature (London) **117**, 514 (1926).
- [52] L. H. Thomas, "The kinematics of an electron with an axis," Philos. Mag. **3**, 1–22 (1927).
- [53] V. Bargmann, Louis Michel, and V. L. Telegdi, "Precession of the polarization of particles moving in a homogeneous electromagnetic field," Phys. Rev. Lett. **2**, 435–436 (1959).
- [54] V. I. Ritus, J. Sov. Laser Res. **6**, 497 (1985).
- [55] V. N. Baier, V. M. Katkov, and V. M. Strakhovenko, Electromagnetic Processes at High Energies in Oriented Single Crystals (World Scientific, Singapore, 1998).
- [56] A. Ilderton, "Note on the conjectured breakdown of qed perturbation theory in strong fields," Phys. Rev. D **99**, 085002 (2019).
- [57] A. Di Piazza, M. Tamburini, S. Meuren, and C. H. Keitel, "Improved local-constant-field approximation for strong-field qed codes," Phys. Rev. A **99**, 022125 (2019).
- [58] C.P. Ridgers, J.G. Kirk, R. Ducloux, T.G. Blackburn, C.S. Brady, K. Bennett, T.D. Arber, and A.R. Bell, "Modelling gamma-ray photon emission and pair production in high-intensity laser-matter interactions," J. Comput. Phys. **260**, 273 – 285 (2014).
- [59] N. V. Elkina, A. M. Fedotov, I. Yu. Kostyukov, M. V. Legkov, N. B. Narozhny, E. N. Nerush, and H. Ruhl, "Qed cascades induced by circularly polarized laser fields," Phys. Rev. ST Accel. Beams **14**, 054401 (2011).
- [60] D.G. Green and C.N. Harvey, "Simla: Simulating particle dynamics in intense laser and other electromagnetic fields via classical and quantum electrodynamics," Computer. Phys. Commun. **192**, 313 – 321 (2015).
- [61] William H. McMaster, "Matrix representation of polarization," Rev. Mod. Phys. **33**, 8–28 (1961).
- [62] Yan-Fei Li, Rashid Shaisultanov, Yue-Yue Chen, Feng Wan, Karen Z. Hatsagortsyan, Christoph H. Keitel, and Jian-Xing Li, "Polarized ultrashort brilliant multi-gev  $\gamma$  rays via single-shot laser-electron interaction," Phys. Rev. Lett. **124**, 014801 (2020).
- [63] F. Wan, Y. Wang, R.-T. Guo, Y.-Y. Chen, R. Shaisultanov, Z.-F. Xu, K. Z. Hatsagortsyan, C. H. Keitel, and J.-X. Li, "High-energy  $\gamma$ -photon polarization in nonlinear breit-wheeler pair production and  $\gamma$ -polarimetry," arXiv: 2020.10346.
- [64] See Supplemental Materials for details on the employed laser fields, on the applied theoretical model, and on the simulation results for other laser or electron parameters.
- [65] V. N. Baier, V. M. Katkov, and V. S. Fadin, Radiation from relativistic electrons (Atomizdat, Moscow, 1973).
- [66] K. Yokoya, CAIN2.42 Users Manual., <https://ilc.kek.jp/~yokoya/CAIN/Cain242/>.
- [67] L. D. Landau and E. M. Lifshitz, The Classical Theory of Fields (Elsevier, Oxford, 1975).
- [68] A. Di Piazza, C. Müller, K. Z. Hatsagortsyan, and C. H. Keitel, "Extremely high-intensity laser interactions with fundamental quantum systems," Rev. Mod. Phys. **84**, 1177–1228 (2012).
- [69] Yousef I. Salamin and Christoph H. Keitel, "Electron acceleration by a tightly focused laser beam," Phys. Rev. Lett. **88**, 095005 (2002).
- [70] W. P. Leemans, A. J. Gonsalves, H.-S. Mao, K. Nakamura, C. Benedetti, C. B. Schroeder, Cs. Tóth, J. Daniels, D. E. Mittelberger, S. S. Bulanov, J.-L. Vay, C. G. R. Geddes, and E. Esarey, "Multi-gev electron beams from capillary-discharge-guided sub-petawatt laser pulses in the self-trapping regime," Phys. Rev. Lett. **113**, 245002 (2014).

- [71] A. J. Gonsalves, K. Nakamura, J. Daniels, C. Benedetti, C. Pieronek, T. C. H. de Raadt, S. Steinke, J. H. Bin, S. S. Bulanov, J. van Tilborg, C. G. R. Geddes, C. B. Schroeder, Cs. Tóth, E. Esarey, K. Swanson, L. Fan-Chiang, G. Bagdasarov, N. Bobrova, V. Gasilov, G. Korn, P. Sasorov, and W. P. Leemans, “Petawatt laser guiding and electron beam acceleration to 8 gev in a laser-heated capillary discharge waveguide,” *Phys. Rev. Lett.* **122**, 084801 (2019).
- [72] A. Narayan, D. Jones, J. C. Cornejo, M. M. Dalton, W. Deconinck, D. Dutta, D. Gaskell, J. W. Martin, K. D. Paschke, V. Tvaskis, A. Asaturyan, J. Benesch, G. Cates, B. S. Cavness, L. A. Dillon-Townes, G. Hays, E. Ihloff, R. Jones, P. M. King, S. Kowalski, L. Kurchaninov, L. Lee, A. McCreary, M. McDonald, A. Micherdzinska, A. Mkrtchyan, H. Mkrtchyan, V. Nelyubin, S. Page, W. D. Ramsay, P. Solvignon, D. Storey, A. Tobias, E. Urban, C. Vidal, B. Waidyawansa, P. Wang, and S. Zhamkotchyan, “Precision electron-beam polarimetry at 1 gev using diamond microstrip detectors,” *Phys. Rev. X* **6**, 011013 (2016).